Effects of Unpaired Bases on the Conformation and Stability of Three-Arm DNA Junctions†

Min Zhong,‡ Michael S. Rashes,‡ Neocles B. Leontis,§ and Neville R. Kallenbach*,‡

Department of Chemistry, New York University, New York, New York 10003, and Department of Chemistry, Bowling Green State University, Bowling Green, Ohio 43403

Received November 5, 1993; Revised Manuscript Received January 11, 1994®

ABSTRACT: Three-arm DNA junctions, in which three double helices intersect at a branch, have unique structure and reactivity of bases at and near the branch. Their solution conformation is asymmetric in the presence of Mg^{2+}, while bases at the branch are sensitive to single-strand-specific agents. Following the surprising report that unpaired bases at the branch stabilize three-arm junctions, we have investigated the geometry and thermodynamics of three-arm junctions containing pendant T and A bases. The results are consistent with additional structure formation in junctions containing up to four pendant bases at the branch: relative to the tight junction, the thermal stability of junctions with two T's or A's at the branch increases; bases near the branch become less reactive to single-strand-reactive probes; and the enthalpy of formation is more negative. The interaction of ethidium observed at the branch in three-arm junctions is enhanced in junctions with unpaired bases at the branch. The geometry of three-arm junctions is perturbed by the presence of pendant bases, as seen by measuring the electrophoretic mobility of junctions to which long duplex arms are appended pairwise.

The conformational repertory of nucleic acids includes states in which three or more duplexes intersect at a single branch point, forming junctions. These three-arm junctions are a common motif in the intramolecular folding of single-strand RNA molecules (Noller, 1984). In the case of DNA, three-arm branched structures arise in T4 phage mutants defective in the gene 49 endonuclease (Minagawa et al., 1983), which cleaves at branches (Kemper, 1991). How deoxy strands differ from RNA in their behavior at branches might provide insight into the structure and thermodynamics of both species of junctions.

Experiments on three-arm "tight" junctions of DNA, that is, structures in which no additional bases are present at the branch, reveal unusual features of the branch site. Electrophoresis experiments on models with pairs of long arms attached to a three-arm unit suggest an asymmetric overall conformation in the presence of Mg^{2+} (Guo et al., 1990). Ethidium bromide binds to three-arm junctions in the vicinity of the branch more tightly than it does to duplex DNA (Lu et al., 1992). Chemical footprinting using a reagent selective for unpaired purines or pyrimidines reveals that bases flanking the branch are more reactive than in duplex DNA. This effect extends up to a full turn of the DNA surrounding the branch site, implying that the formation of three-arm junctions imposes strain of some kind (Duckett & Lilley, 1990; Guo et al., 1990). The geometry of a three-arm junction is determined by the sequence of bases that flank the branch as well as those next to them (Lu et al., 1991). Other experimental evidence indicates that the three-arm junction is relatively flexible with respect to bending or twisting around the branch (Ma et al., 1986; Jensch & Kemper, 1986).

Introduction of a very short "duplex" arm into a longer DNA duplex disrupts base pairs in the duplex (Zhong & Kallenbach, 1993). Together with data on the geometry and stability of these DNA "necks", this has suggested a dynamical model for tight three-arm junctions: each of the base pairs flanking the branch can break transiently, allowing the bases to associate with the remaining "duplex". We envisage this as partial intercalation of the liberated base into the adjacent duplex, although this mechanism is not proven. The result would be a manifold of intrinsically dynamic, interconverting substates in a three-arm junction, as each pair of arms forms the duplex in this model. This picture has been used to describe the effect of introducing T·T mismatches at sites flanking a three-arm junction (Zhong et al., 1993).

The observation that unpaired bases at the branch of a three-arm junction stabilize the structure (Leontis et al., 1991) can also be rationalized by the dynamical model. The population of conformational substates that make up the tight junction collapses, and a smaller set of structures results. What is actually observed in NMR experiments is consistent with an overall Y-shaped structure (Leontis et al., 1993; Rosen & Patel, 1993a,b), in which unique stacking arrangements of the pendant bases can be seen at the branch. In the case of pyrimidines, the unpaired bases appear to be relatively exposed to solvent. The NMR results provide little detailed information about the substates that may be present, or what the overall geometry may be. Furthermore, the perturbing effect of bulged bases on the junction conformation is not determined in those experiments. In order to address these questions, we have investigated the conformational and thermodynamic properties of a series of three-arm junctions containing unpaired T*n* and A*n* (n = 1–4) bases at the branch (Figure 1). The tight three-arm junction with arms of identical sequences, X being absent, is used as a reference in the present study.

MATERIALS AND METHODS

Synthesis and Purification of Oligonucleotides. Oligonucleotides used in this study were synthesized on an automated

† This research was supported by Grant CA24101 from the National Cancer Institute of the NIH (to N.R.K.), U.S. Public Health Service Grant GM 41454 (to N.B.L.), Petroleum Research Fund Grant 20871-GB4 (to N.B.L.), and Research Corporation Grant C-2314 (to N.B.L.).

* Author to whom correspondence should be addressed.

‡ New York University.

§ Bowling Green State University.

® Abstract published in *Advance ACS Abstracts,* March 1, 1994.

0006-2960/94/0433-3660$04.50/0 © 1994 American Chemical Society

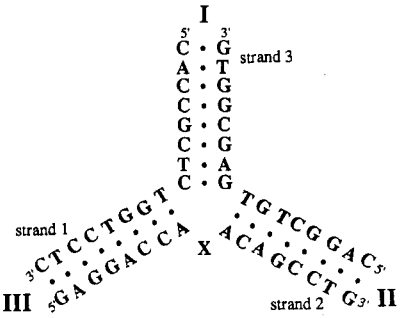

Junction Name	X
Y1	None
YA	A
YAA	AA
YAAA	AAA
YAAAA	AAAA
YT	T
YTT	TT
YTTT	TTT
YTTTT	TTTT

FIGURE 1: Sequences and schematic representations of the nine synthetic DNA three-arm junctions used in this study. Each molecule consists of two common 16-mer strands (strands 1 and 3) and one strand with 0–4 A's or T's inserted at the middle (strand 2). The strand numbering indicated in this figure is used throughout the text.

DNA synthesizer, deprotected by routine phosphoramidite procedures (Caruthers, 1982), and purified by ion-exchange HPLC or polyacrylamide gel electrophoresis. 5′-Terminal labeling used bacteriophage T4 polynucleotide kinase (Bethesda Research Laboratories) and [γ-^{32}P]ATP; the labeled strands were purified by polyacrylamide gel electrophoresis. The concentration of strands in stock solutions was determined spectrophotometrically at 260 nm and 80 °C, using the nearest-neighbor values of Cantor et al. (1970).

Annealing Reactions. These were carried out by mixing stoichiometric concentrations of the appropriate DNA strands in 50 mM Tris·HCl (pH 7.5) with 10 mM $MgCl_2$ or 100 mM NaCl, heating at 90 °C for 2 min, cooling slowly to room temperature, and finally chilling to 4 °C.

Gel Electrophoresis. Unless otherwise indicated, native polyacrylamide (19:1 monomer/bis ratio) gels were run in buffer that contained 40 mM Tris and 20 mM acetic acid with 2 mM $MgCl_2$ (pH 8.1) or 20 mM NaCl at 4 °C. Gels were stained by Stains-All or exposed to X-ray film. For denaturing gels, the products of cleavage reactions were run on 20% polyacrylamide (19:1 monomer/bis ratio)/7 M urea gels at 40 °C. Gels were dried and exposed to X-film at −70 °C using an intensifying screen.

Elongation of DNA Molecules. The 60-bp DNA reporter fragment with natural sequence used in this study is formed by mixing stoichiometric concentrations of a synthetic 58-nucleotide strand with a complementary 5′-phosphorylated 62-nucleotide strand. The reporter duplex thus contains a blunt end with a 4-base, 5′ overhang that is *Eco*RI-derived. Elongation of branched DNAs containing a pseudo-*Eco*RI end is achieved by ligation to the synthetic reporter fragment, as described by Cooper and Hagerman (1987, 1989). Ligation reactions with T4 DNA ligase (Bethesda Research Laboratories) were carried out in 50 mM Tris·HCl (pH 7.5), 10 mM $MgCl_2$, 1 mM ATP, and 1 mM dithiothreitol at 16 °C overnight. Following heat inactivation (65 °C for 5 min), ligase was removed by phenol extraction and DNA was precipitated by ethanol.

Elongated branched DNA halves or extended branched DNAs were purified on 6% polyacrylamide gels.

UV Melting Curves. Absorbance versus temperature profiles (melting curves) for the DNA molecules, at 3.75 μM total strand concentrations in a 20 mM sodium phosphate buffer containing 100 mM NaCl and 2 mM $MgCl_2$ or 2 mM EDTA (pH 7.0), were recorded at 260 nm on a thermoelectrically controlled Perkin-Elmer 552 spectrophotometer. The temperature was scanned at a heating rate of 1 °C/min. These melting curves allow us to measure the transition temperatures, T_m, the midpoints of the order–disorder transition of these DNA molecules (Marky & Breslauer, 1987).

Differential Scanning Calorimetry. The total heat of the helix–coil transition of each DNA molecule was measured directly with a Microcal MC-2 differential scanning calorimeter (DSC). A typical solution for DSC experiments contained 20 mM sodium cacodylate, 100 mM NaCl, and 1 mM $MgCl_2$ (pH 7.0), with a total strand concentration of 0.3 mM, and was scanned from 5 to 90 °C at a heating rate of 45 °C/h. Buffer alone was used as a blank; a buffer versus buffer scan was subtracted from the sample scan and normalized for the heating rate. The area of the resulting curve is proportional to the transition heat; normalized for the number of moles, this heat gives the transition enthalpy ($\Delta H°_{cal}$). The DSC curves also allow one to estimate the transition entropy ($\Delta S°$) and free energy ($\Delta G°$) from the area of $\Delta C_p/T$ versus T with the Gibbs equation, respectively.

Osmium Tetraoxide Modification. DNA samples (10 μM) were incubated with 1 mM osmium tetraoxide (OsO_4) and 3% pyridine in 50 mM Tris·HCl (pH 7.5) with 10 mM $MgCl_2$ at 4 °C for 10 min (Lilley & Palecek, 1984). Reactions were stopped by two sequential ethanol precipitations, and the mixes were lyophilized. The DNAs were cleaved at the site of reaction by treatment with 100 μL of 1 M piperidine at 90 °C for 30 min and lyophilized.

Diethyl Pyrocarbonate Modification. Branched DNAs were modified by diethyl pyrocarbonate (DEPC) essentially as described by Herr (1985). DNAs (10 μM) were suspended in 10 μL of 50 mM Tris·HCl (pH 7.5) with 10 mM $MgCl_2$ and incubated with 1 μL of DEPC for 60 min at 4 °C. The reactions were terminated by two sequential rapid ethanol precipitations and then lyophilized. The DNAs were cleaved at the sites of DEPC modification by treatment with 100 μL of 1 M piperidine at 90 °C for 30 min and lyophilized.

MPE·Fe^{II} Cleavage Reaction. DNA samples (10 μM) were exposed to 10 μM Fe^{II} and 10 μM MPE (van Dyke & Dervan, 1983) in a buffer containing 10 mM Tris·HCl (pH 7.5) with 50 mM NaCl and 10 mM $MgCl_2$ for 15 min at 4 °C, followed by the addition of 4 mM dithiothreitol for 60 min. The reaction was stopped by rapid ethanol precipitation and lyophilized.

Sequencing Reaction. Purine-specific (A+G) sequencing ladders were generated from each 5′-^{32}P-labeled oligonucleotide using the piperidine–formate reaction (Maxam & Gilbert, 1980).

Densitometry. Autoradiograms were scanned on a Hoefer GS300 densitometer, without base-line corrections.

RESULTS

Formation of Three-Arm Junctions. For any synthetic model junction, it is essential to establish that the strands interact with appropriate stoichiometry to form the anticipated complexes (Kallenbach et al., 1983). To do this, we carried out polyacrylamide gel electrophoresis under native nondenaturing conditions. Figure 2 shows the results of electrophoretic analysis of single strands, equimolar mixtures of dimers, and trimers formed by the strands designated in Figure 1, detected using the dye, Stains-All, which is sensitive to both single strands and multistrand complexes. Strand 1 (lanes a and h) migrates more rapidly than the mixture of strands 1 + 2 (lanes b and i), while the three-strand combinations (lanes c–g and j–n) all form single, discrete bands with lower mobility than the 1 + 2 dimer. A progressive reduction in mobility is also seen as the number of unpaired bases in the X sequence increases, for both the T and A series. This is the behavior anticipated for a series of nucleic acid chains of similar

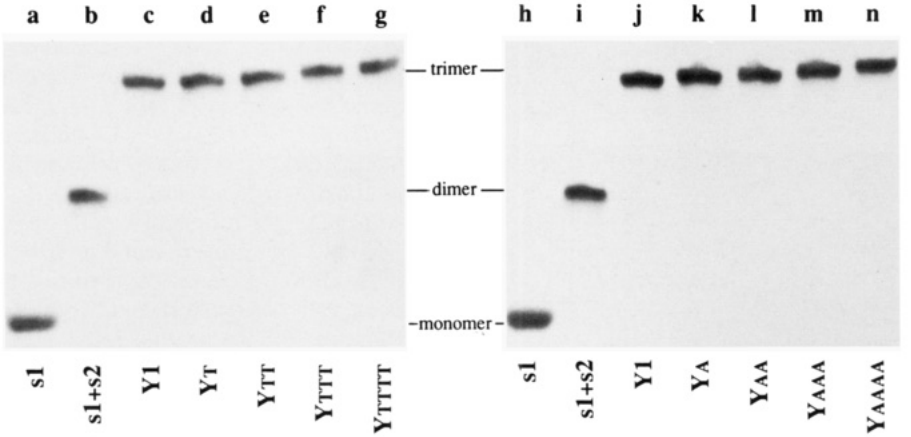

FIGURE 2: Polyacrylamide gel electrophoresis (20%) of oligodeoxynucleotide strands and mixtures. A photograph of a native gel is shown, in which the junction components have been combined in equimolar combinations to illustrate their association under conditions of electrophoresis. Each lane contains 3.0 μg of each strand alone or in combination with others. The numbering convention refers to that of Figure 1.

conformations and increasing chain length; no major conformational change or evidence for strand dissociation is indicated.

Chemical Reactivity of Bases in the Vicinity of the Branch. Monitoring the accessibility of the strands in three-arm junctions to single-strand-reactive probes has provided important information concerning the state of base pairing at the branch (Guo et al., 1990). The reagent OsO_4 is selective for T (Lilley & Palecek, 1984), and DEPC attacks purines (Herr, 1985), in the single-strand state. Figure 3A shows the "footprint" (Galas & Schmitz, 1978) resulting from exposure of the series of three-arm junctions in Figure 1 to OsO_4, followed by hydrolysis of the reacted chains with piperidine. The center panel, with strand 2 labeled in each junction, monitors the presence of 1–4 T's in this strand, except in Y1. The left and right panels indicate strong reactivity of the T's flanking the branch in strands 1 (T9) and 3 (T8) of Y1 (see Figure 1), relative to the full-duplex control, labeled ds. The reactivity of both of these thymines is reduced as T's are added to strand 2, which is consistent with stabilization of the flanking base pairs in the junction. The piperidine treatment leads to apparent reactivity in non-thymine sites adjacent to the strongly reactive thymines in Y1 (Figure 3A); this effect has been interpreted as indicative of opening base pairs in the arms bordering the branch (Lu et al., 1991). The effect is sharply reduced in the junctions containing excess bases. In strand 3, reactivity at G7 next to T8 follows a pattern parallel to that of T8 itself.

Similar results are obtained using DEPC, which monitors exposed purines, principally A's (Herr, 1985). In addition to the A's flanking the branch, the added A's are sensitive to DEPC. One G residue flanking the branch, G9, also is reactive. Figure 3B indicates the sites in Y1, YTT, and YAA that are labile to OsO_4 and DEPC.

MPE·Fe^{II} Cleavage Patterns. A common feature in all branched DNAs studied so far is the strong interaction of intercalative molecules at the branch (Lu et al., 1992). This effect is demonstrated most readily by the use of Dervan's MPE·Fe^{II} reagent, which cleaves DNA in the vicinity of ethidium binding sites (van Dyke & Dervan, 1983). In both three- and four-arm junctions, preferential interaction of ethidium at the branch is detected as enhanced reactivity for MPE·Fe^{II}, which is competitively inhibited by ethidium [see Lu et al. (1992)]. Densitometer traces of autoradiograms of PAGE experiments in which junctions with labeled strands have been exposed to MPE·Fe^{II} are shown in Figure 4A. Relative to a fully duplex control, in Y1 strong enhancement of reactivity occurs at a series of positions flanking the branch: 8–11 in strand 1, 9–12 in strand 2, and 10–12 in strand 3. In each of the junctions with additional bases at the branch, enhanced reactivity to MPE·Fe^{II} relative to the levels in Y1 is observed on all three strands. Sites of enhanced reactivity are indicated schematically in Figure 4B, imposed on the sequence of the representative species Y1, YTT, YAA, and YAAAA. Both the amplitude and extent of enhanced reactivity increase, consistent with tighter binding and/or increased stoichiometry. The difference in behavior between bulged T's and A's is worthy of note: the A's are all sites of enhanced scission, while the T's are not. This indicates a fundamental difference in how these complexes bind ethidium.

Conformational Analysis of Representative Junctions with Reporter Arms by PAGE. An experimental protocol for investigating the conformation of branched DNA molecules has been introduced by Cooper and Hagerman (1987): pairs of reporter arms close to one persistence length in size are appended to the junction to be studied, and the relative mobilities of these are determined in native PAGE. The reasoning is that each pair defines an effective set of valence angles between the probe duplexes, and the electrophoretic mobility of DNA molecules in this size range is sensitive to bends in the helix axes (Hagerman, 1984, 1985; Koo et al., 1986). In the simplest case, the extent of retardation is related to the magnitude of the bend angle, allowing assessment of the effective angle between pairs of arms in DNA junctions (Cooper & Hagerman, 1987; Duckett et al., 1988; Guo et al., 1990).

Figure 5A summarizes the experiment as it applies to three-arm junctions. Reporter fragments of 60 bp are ligated pairwise to form three complexes of identical size, as shown. Differences in mobility among these can then be attributed to differences in the effective valence angle between the arms of the junction or in the distribution of angles, if there is population heterogeneity. In the case of a completely symmetric or floppy junction, the mobility of each pair of strands should be the same in the case of Y1 and similar in the junctions with an elongated strand. Figure 5B shows the results of this analysis for the four junctions, Y1, YTT, YAA, and YAAAA, in the presence of Mg^{2+}. In Y1, the complexes designated b and c migrate at nearly the same rate, more slowly than a. In the junctions containing unpaired bases, the most apparent difference is that complex c has higher mobility

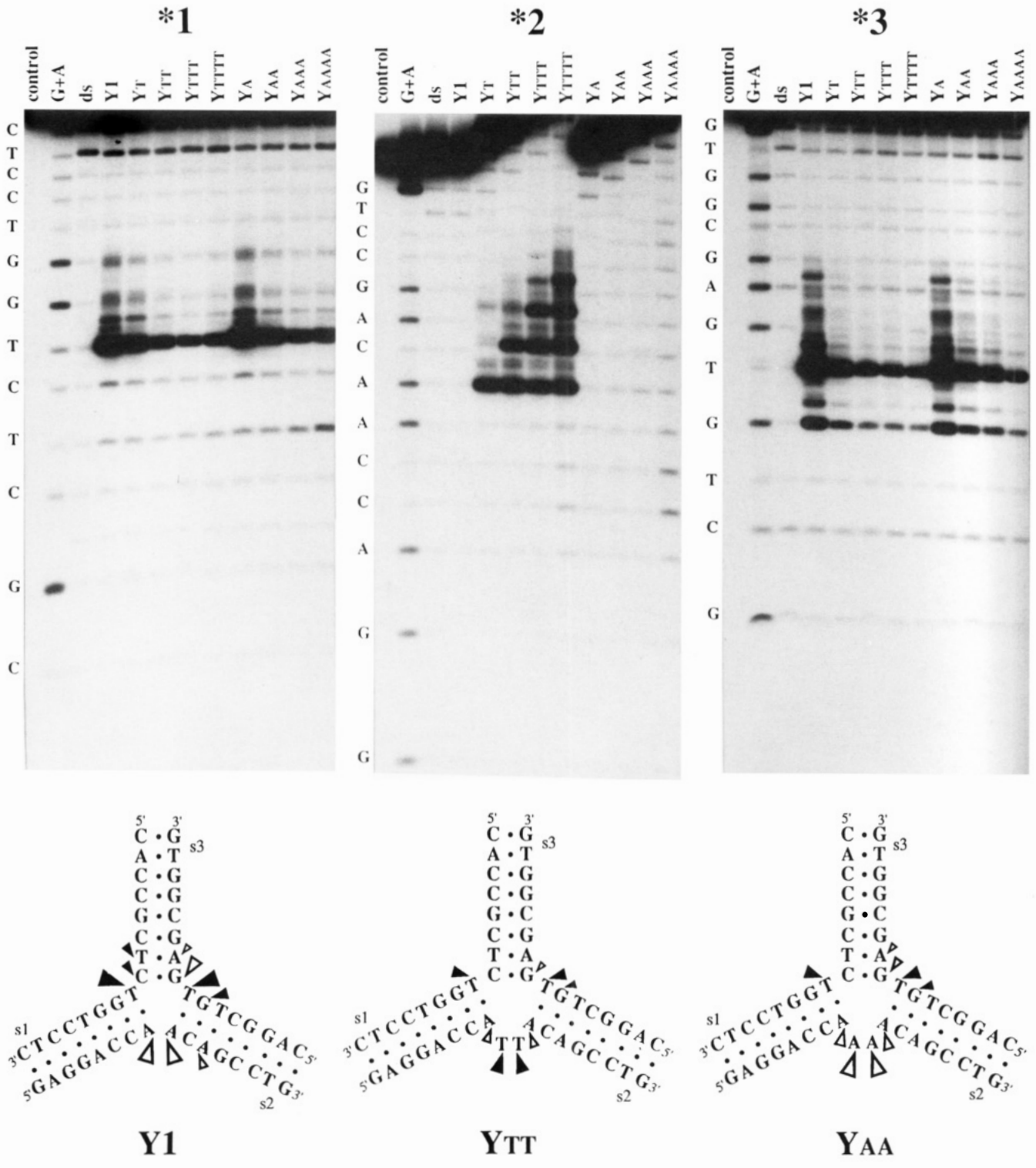

FIGURE 3: (A, top) Osmium tetraoxide–piperidine cleavage reactions. Junctions 5′-labeled with ^{32}P were cleaved with OsO_4–piperidine as described in Materials and Methods and electrophoresed on a denaturing gel along side A + G sequence markers derived from the same radioactive strand. Note that T9 in strand 1 and T8G9 in strand 3 of bulged junctions are less reactive relative to those of Y1. (B, bottom) Schematic representations of the results of OsO_4 and DEPC reactivity in three junctions. The sequences of Y1, YTT, and YAA are shown, with preferential sites of OsO_4 reactivity indicated by filled arrows and DEPC reactivity by open arrows.

than in Y1. A second difference is broadening of the band corresponding to complex b in YAA and YAAAA. The patterns in the absence of Mg^{2+} do not indicate symmetry in geometry (Figure 5C), and the broadening in complex b is still present. Figure 6 shows that, at higher temperature, the broadening of the band corresponding to complex b for YAA and YAAAA resolves into two distinct bands. There is thus conformational heterogeneity present in both junctions with unpaired purines, but not in YTT. Figure 5D illustrates an interpretation of the mobility differences observed in the absence and presence of Mg^{2+}.

Thermodynamics of Junctions with Unpaired Bases. The stability of Y1 and the junctions containing unpaired bases at the branch was evaluated by optical melting experiments. The results in Table 1 show that, at the same concentration of strands, the midpoint of the thermal denaturing transition

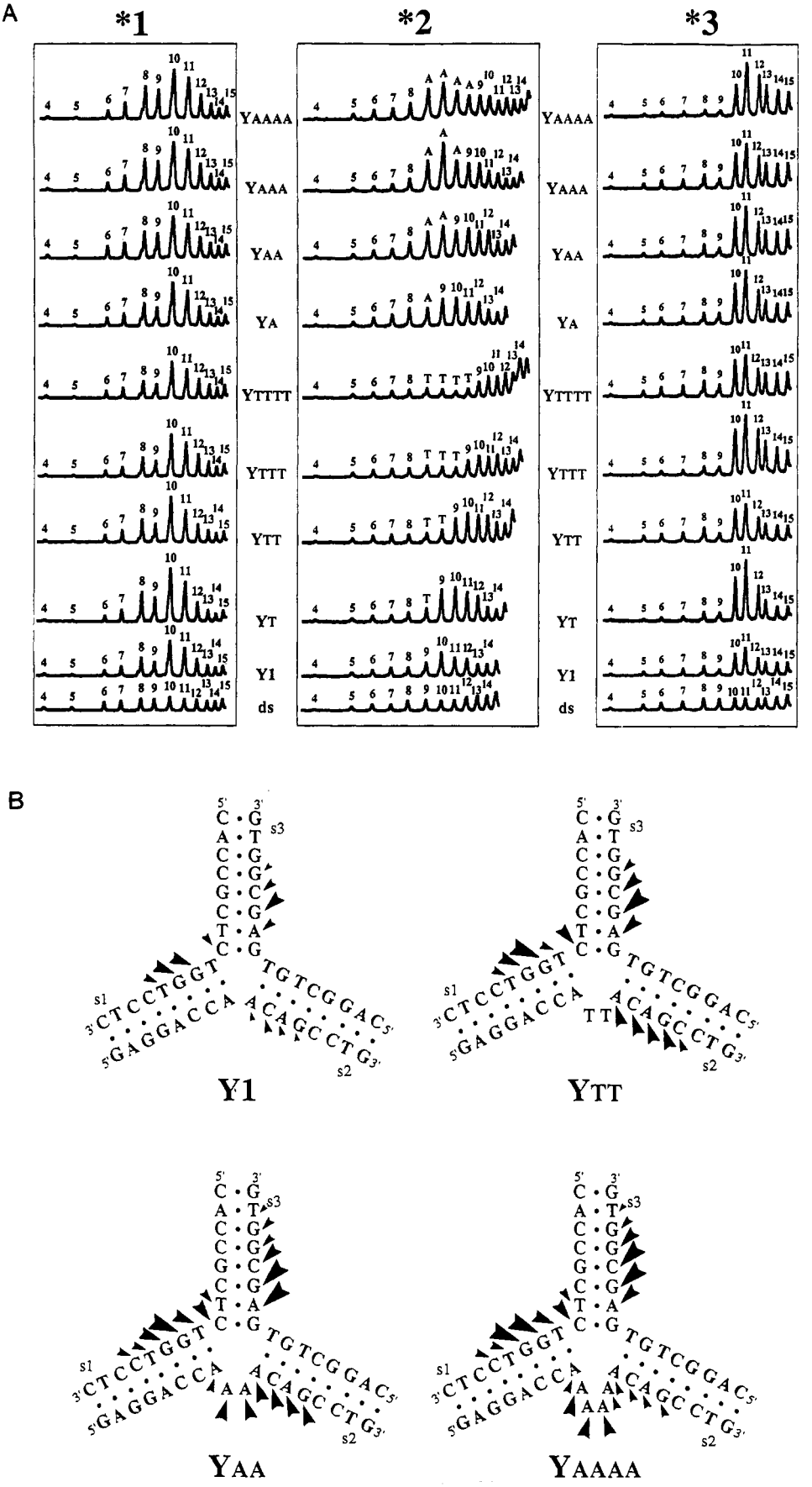

FIGURE 4: Cleavage of junctions by MPE·Fe^{II}. (A, top) Densitometric scans of the cleavage patterns of junctions due to MPE·Fe^{II}. Each panel of this figure corresponds to a given strand of junctions and contains 10 scans, each corresponding to one of the junctions or duplexes of this study. The branch point lies between positions 8 and 9 on each strand. Note that enhancement of cleavage near branch sites is seen in all bulged junctions relative to Y1, and stronger enhancement of cleavage is seen near A bulges relative to T bulges. (B, bottom) Sites of preferential cleavage by MPE·Fe^{II} in junctions Y1, YTT, YAA, and YAAAA are compared to those in the duplex. The size of the arrows is a measure of the quantitative intensity of each responsive site.

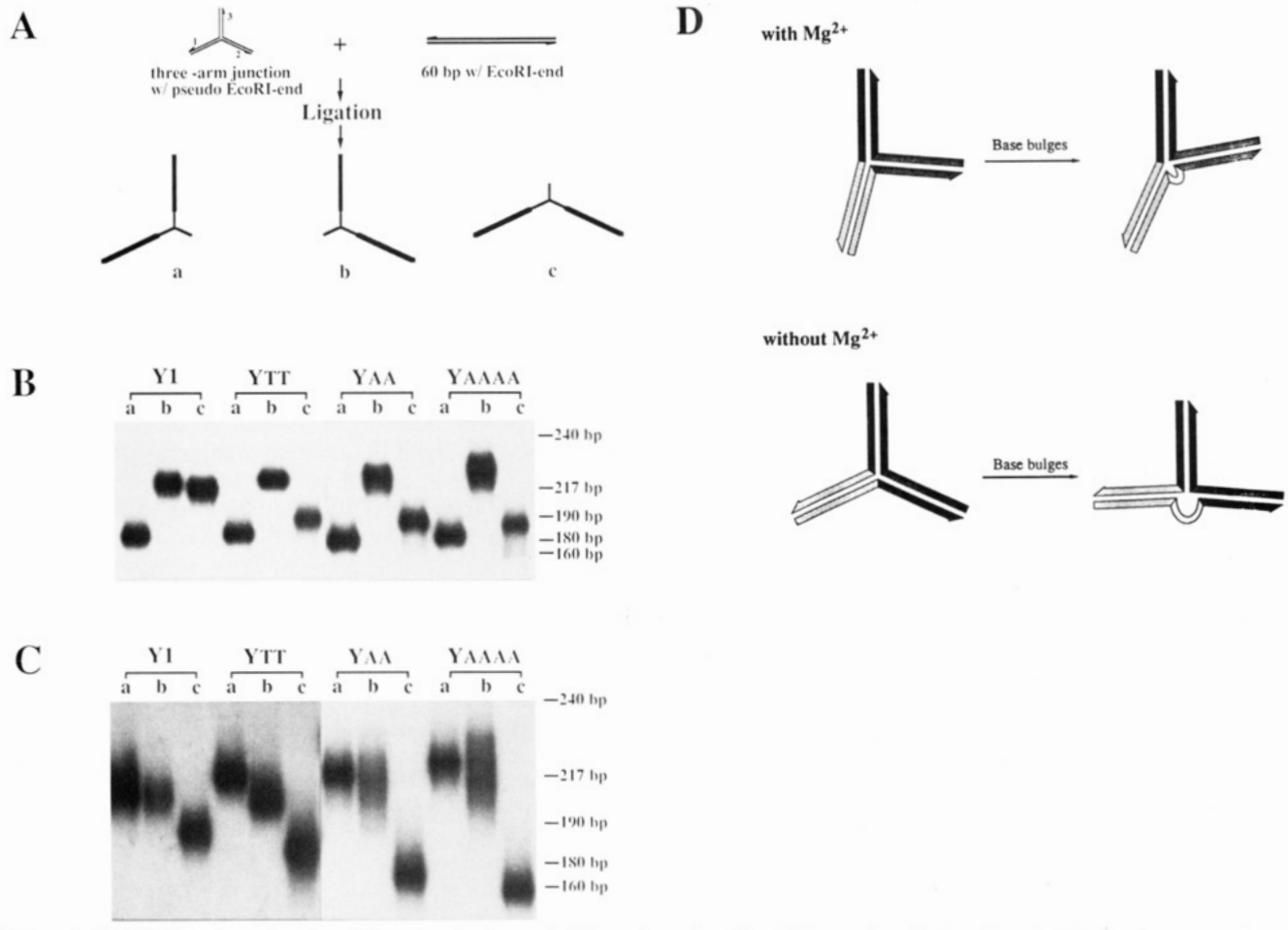

FIGURE 5: (A) Outline of construction of three species for analysis by polyacrylamide gel electrophoresis. A radioactively labeled DNA junction with two pseudo-*Eco*RI ends is ligated to the *Eco*RI-ended reporter fragment (Cooper & Hagerman, 1987). (B) 12% Gel electrophoretic analysis of DNA junctions with two arms extended in the presence of Mg^{2+}. The ordering of these samples is the same as in A. (C) Mobility of DNA junctions with two arms extended in the absence of Mg^{2+}. (D) Schematic interpretations of the results from gel electrophoretic analysis.

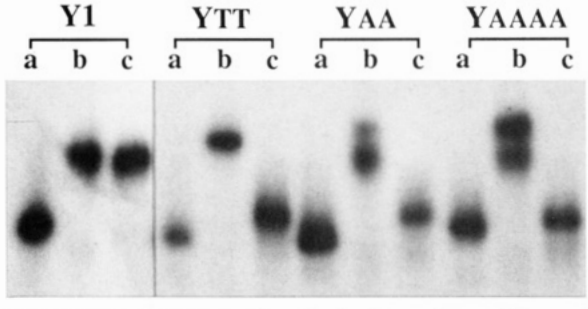

FIGURE 6: Gel electrophoretic analysis of complexes with reporter arms at 25 °C. The complexes identified in Figure 5 were run in 12% nondenaturing PAGE at 25 °C, in the presence of Mg^{2+}. Complex b shows two bands at this temperature, rather than the single broadened band at 4 °C (Figure 5B).

increases as 1–3 T or A residues are added at the branch. The stability is maximal for YTT and YAA and decreases until the junctions with four unpaired bases are less stable than Y1. To determine the basis for these stability effects, we carried out differential scanning calorimetry experiments on the four junctions listed in Table 2. We have shown previously that Y1 is destabilized relative to duplex DNA 16-mers, via a reduction in both the enthalpy and entropy contributions (Zhong et al., 1993). The DSC profiles for Y1, YTT, YAA, and YAAAA are shown in Figure 7, and the results are summarized in Table 2. The enthalpies of formation of YTT and YAA are both higher than that of Y1, while that of YAAAA is lower. This increase in enthalpy is consistent with the base stacking seen in NMR experiments (Leontis et al., 1993; Rosen & Patel, 1993a,b). The NMR data have not detected H-bonding of these bases, although the enthalpy contribution and electrophoretic mobility data are suggestive of pairing interactions. The entropy differences between Y1 and YTT or YAA are small, while in YAAAA we observe a large reduction in the entropy contribution to the free energy. This is consistent with a loop entropy effect.

Table 1: Transition Temperatures of Junctions[a]

junction	T_m (°C) w/Mg^{2+}	T_m (°C) w/o Mg^{2+}
Y1	38.9	35.3
YT	40.0	36.7
YTT	40.4	36.8
YTTT	39.8	35.5
YTTTT	38.1	33.9
YA	39.3	36.1
YAA	40.1	36.5
YAAA	39.8	36.2
YAAAA	38.5	34.2

[a] Absorbance versus temperature profiles (melting curves) were measured at 3.75 μM total DNA strand concentration in a 20 mM sodium phosphate buffer containing 100 mM NaCl and 2 mM $MgCl_2$ or 2 mM EDTA (pH 7.0).

DISCUSSION

The above data confirm the fact that adding two unpaired bases to the branch in the three-arm junction Y1 stabilizes the structure. The junction we are studying is different in

Table 2: Thermodynamic Parameters for Junction Formation at 20 °C[a]

junction	$\Delta H°_{cal}$ (kcal/mol)	$\Delta\Delta H°_{cal}$ (kcal/mol)	$\Delta G°$ (kcal/mol)	$T\Delta S°$ (kcal/mol)
Y1	−156		−15	−141
YTT	−160	−4	−16	−144
YAA	−161	−5	−16	−145
YAAAA	−133	23	−13	−120

[a] All measurements were taken in 20 mM sodium cacodylate buffer containing 100 mM NaCl and 1 mM $MgCl_2$ at pH 7.0. The $\Delta H°_{cal}$ values are averages of five determinations and are within ±3%; the $T\Delta S°$ values are within 5% experimental error. The $\Delta\Delta H°_{cal}$ values are relative to the corresponding enthalpies for Y1.

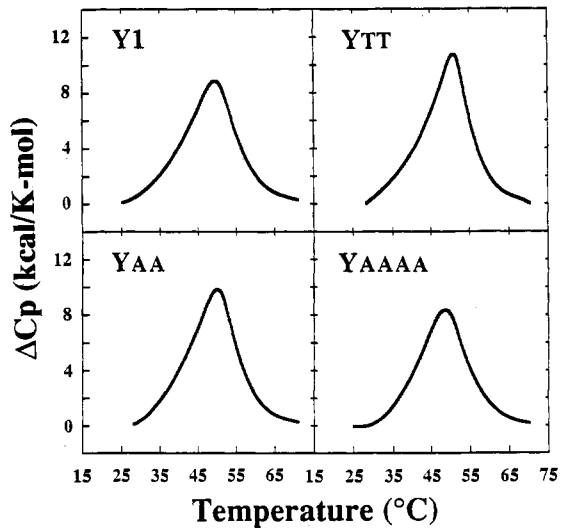

FIGURE 7: Differential heat absorption profiles (DSC) for Y1 and the bulged junctions in 20 mM sodium cacodylate buffer containing 100 mM NaCl and 1 mM $MgCl_2$ (pH 7.0).

sequence from those used by Leontis et al. (1991) or Rosen and Patel (1993a,b), so that the effect is a general one. One or three unpaired bases stabilize the junction as well, but to a lesser extent, while four unpaired bases are destabilizing. Our results shed light on several aspects of the stabilizing and destabilizing effects. First, the overall conformation of the junctions changes. As seen in Figure 5B, the relative mobilities of complexes a and b are fairly insensitive to the presence of the added bases; on the other hand, the mobility of complex c increases significantly. Trigonal models in which two arms intersect at an obtuse angle, while the third is folded tightly, can account for this, and such structures have been proposed from NMR studies (Rosen & Patel, 1993a,b).

The mobility of complex a in Figure 5B, which has the highest mobility, is lower than that of a duplex of 180 bp, implying retardation due to the short arm, angular bending, or both. All complexes formed from the junction YTT show single bands on nondenaturing PAGE. Junctions with additional A's show more complicated electrophoretic behavior: complex b is broader than a or c at low temperature and resolves into two bands with different mobilities as the temperature increases (Figure 6). This might reflect a population of different states at the higher temperature or possibly be a consequence of larger scale motions of the arms with respect to each other. NMR analysis of the structure of a junction with two T's added at the branch (Leontis et al., 1993) indicates a Y-shaped geometry, in which the T's are stacked at the branch. Whether or not the T's are H-bonded as well is not clear at this point. The conclusion we can reach from these experiments is that the stability of a "tight" three-arm junction is enhanced by the addition of two bases at the branch, via an increase in the enthalpy of formation of 4–5 kcal/mol, which is partially compensated by an increase in entropy. The resulting net change in $\Delta G°$ is small, around 1 kcal/mol.

Changes in the conformation of the junction as bases are added can be detected by differences in the relative mobilities of complexes in which pairs of arms have been extended with reporter duplexes (Cooper & Hagerman, 1987). The most striking effect seen is the broadening of the mobility of the b complexes in the case of YAA and YAAAA and the splitting observed at higher temperature. The fact that this is not seen in YTT underscores the fact that the structure with pyrimidines pendant must differ considerably from that with purines. This is also clear from the difference in MPE·Fe^{II} scission patterns between the T and A bulged species (Figure 4B). At higher temperature, splitting of the bands of YAA and YAAAA into two can be seen (Figure 6). This points to the fact that the structure of the complex with appended bases is not unitary.

As we have emphasized in our analysis of the tight three-arm junction and neck complexes (Zhong & Kallenbach, 1993), the three-arm junction has a dynamic conformational structure, which we have interpreted in terms of a population of interconverting substates. It is interesting that, despite the stabilizing presence of the base pairs formed from the added bases, the geometry remains consistent with multistate behavior. A variety of models can be constructed for different isomeric states of a junction containing added base pairs at the branch and for the electrophoretic consequences of these (see Figure 5D). The nature of the process responsible for the bands that resolve in Figure 6 is thus an obvious problem for investigation. In addition, one would like to know how the structure and dynamics of these systems depend on the actual sequence of bases flanking the branch.

ADDED IN PROOF

Studies of related bulged three-way DNA junctions were recently reported by Welch et al. (1993).

REFERENCES

Cantor, C., Warshaw, M. W., & Shapiro, H. (1970) *Biopolymers 9*, 1059–1077.
Caruthers, M. H. (1982) in *Chemical and Enzymatic Synthesis of Gene Fragments* (Gassen, H. G., & Lang, A., Eds.) pp 71–79, Verlag Chemie, Weinheim, Germany.
Cooper, J. P., & Hagerman, P. J. (1987) *J. Mol. Biol. 198*, 711–719.
Cooper, J. P., & Hagerman, P. J. (1989) *Proc. Natl. Acad. Sci. U.S.A. 86*, 7336–7340.
Duckett, D. R., & Lilley, D. M. J. (1990) *EMBO J. 9*, 1659–1664.
Duckett, D. R., Murchie, A. I. H., Diekmann, S., von Kitzing, E., Kemper, B., & Lilley, D. M. J. (1988) *Cell 55*, 79–89.
Galas, D. J., & Schmitz, A. (1978) *Nucleic Acids Res. 3*, 3157–3170.
Guo, Q., Lu, M., Churchill, M. E. A., Tullius, T. D., & Kallenbach, N. R. (1990) *Biochemistry 29*, 10927–10934.
Hagerman, P. J. (1984) *Proc. Natl. Acad. Sci. U.S.A. 81*, 4632–4636.
Hagerman, P. J. (1985) *Biochemistry 24*, 7033–7037.
Herr, W. (1985) *Proc. Natl. Acad. Sci. U.S.A. 82*, 8009–8013.
Jensch, F., & Kemper, B. (1986) *EMBO J. 5*, 181–189.
Kallenbach, N. R., Ma, R.-I., & Seeman, N. C. (1983) *Nature 305*, 829–831.
Kemper, B., Pottmeyer, S., Solaro, P., & Kosak, H. (1991) in *Structure and Methods* (Sarma, R. H., & Sarma, M. H., Eds.)

Vol. 1, pp 215–230, Adenine, New York.
Koo, H.-S., Wu, H.-M., & Crothers, D. M. (1986) *Nature 320*, 501–506.
Leontis, N. B., Kwok, W., & Newman, J. S. (1991) *Nucleic Acids Res. 19*, 759–766.
Leontis, N. B., Hills, M. T., Piotto, M., Malhotra, A., Nussbaum, J., & Gorenstein, D. G. (1993) *J. Biomol. Struct. Dyn. 11*, 215–223.
Lilley, D. M. J., & Palecek, E. (1984) *EMBO J. 3*, 1187–1192.
Lu, M., Guo, Q., & Kallenbach, N. R. (1991) *Biochemistry 30*, 5815–5820.
Lu, M., Guo, Q., & Kallenbach, N. R. (1992) *Crit. Rev. Biochem. Mol. Biol. 27*, 157–190.
Ma, R.-I., Kallenbach, N. R., Sheardy, R. D., Petrillo, M. L., & Seeman, N. C. (1986) *Nucleic Acids Res. 14*, 9745–9753.
Marky, L. A., & Breslauer, K. J. (1987) *Biopolymers 26*, 1601–1620.
Maxam, A. M., & Gilbert, W. (1980) *Methods Enzymol. 65*, 499–560.
Minagawa, T., Murakami, A., Ryo, Y., & Yamagishi, H. (1983) *Virology 126*, 183–193.
Noller, H. F. (1984) *Annu. Rev. Biochem. 53*, 119–162.
Rosen, M. A., & Patel, D. J. (1993a) *Biochemistry 32*, 6563–6575.
Rosen, M. A., & Patel, D. J. (1993b) *Biochemistry 32*, 6576–6587.
van Dyke, M. W., & Dervan, P. B. (1983) *Nucleic Acids Res. 11*, 5555–5567.
Welch, J. B., Duckett, D. R., & Lilley, D. M. J. (1993) *Nucleic Acids Res. 31*, 4548–4555.
Zhong, M., & Kallenbach, N. R. (1993) *J. Mol. Biol. 230*, 766–778.
Zhong, M., Rashes, M. S., & Kallenbach, N. R. (1993) *Biochemistry 32*, 6898–6907.